1894 Biophysical Journal Volume 85 September 2003 1894–1902

The Dead-End Elimination Method, Tryptophan Rotamers, and Fluorescence Lifetimes

Mario Hellings,* Marc De Maeyer,† Stefan Verheyden,* Qiang Hao,‡ Els J. M. Van Damme,§
Willy J. Peumans,¶ and Yves Engelborghs*
*Laboratory of Biomolecular Dynamics, Catholic University of Leuven, Heverlee, Belgium; †Laboratory of Biomolecular Modelling, Catholic University of Leuven, Heverlee, Belgium; ‡Institute of Biosciences and Technology, Texas A&M University, System Health Sciences Center, Houston, Texas; §Department of Molecular Biotechnology, University of Ghent, Ghent, Belgium; and ¶Laboratory of Phytopathology and Plant Protection, Catholic University of Leuven, Heverlee, Belgium

ABSTRACT The Dead-End Elimination method was used to identify 40 low energy microconformations of 16 tryptophan residues in eight proteins. Single Trp-mutants of these proteins all show a double- or triple-exponential fluorescence decay. For ten of these lifetimes the corresponding rotameric state could be identified by comparing the bimolecular acrylamide quenching constant (k_q) and the relative solvent exposure of the side chain in that microstate. In the absence of any identifiable quencher, the origin of the lifetime heterogeneity is interpreted in terms of the electron transfer process from the indole Cε3 atom to the carbonyl carbon of the peptide bond. Therefore it is expected that a shorter [Cε3-C=O] distance leads to a shorter lifetime as observed for these ten rotamers. Applying the same rule to the other 30 lifetimes, a link with their corresponding rotameric state could also be made. In agreement with the theory of Marcus and Sutin, the nonradiative rate constant shows an exponential relationship with the [Cε3-C=O] distance for the 40 datapoints.

INTRODUCTION

Fluorescence studies of proteins often provide useful information regarding the environment and the dynamics of the region surrounding naturally occurring fluorescent amino acids like tryptophan. However, this necessitates an exact knowledge of the relation between the fluorescent properties and the protein environment. This is often problematical because the fluorescence decay of a single tryptophan residue in a protein is usually multiexponential. This multiexponential decay is either the consequence of excited state reactions or of the existence of different tryptophan microconformations (Szabo and Rayner, 1980; Bajzer and Prendergast, 1993; Brown and Royer, 1997; Dahms et al., 1995; Ababou and Bombarda, 2001). Hudson proposed a model that involves reversible ionization of the excited tryptophan residue due to collisional transfer of an electron to a neighboring residue (Hudson, 1999). Other groups have also suggested the involvement of an electron transfer process as the principal quenching mechanism in proteins and peptides (Antonini et al., 1997; Chen and Barkley, 1998; Ababou and Bombarda, 2001). In the absence of quenching side chains, the carbonyl group of the peptide itself is thought to be the responsible quencher (Ricci and Nesta, 1976; Chen et al., 1996; Adams et al., 2002). The carbonyl group of the peptide itself will act as an acceptor with the indole Cε3 atom of tryptophan as donor (Sillen et al., 2000). According to Milner-White (1997), the carbon of the peptide carbonyl contains a net-positive charge, and is therefore available to accept an electron. The dependency of electron transfer on the distance between the acceptor and the donor, as well as on the medium in between, are supposed to be responsible for different lifetimes for different rotamer positions of tryptophan (Chang et al., 1983; Goldman et al., 1995; Sillen et al., 2000; Ababou and Bombarda, 2001; Adams et al., 2002).

Sillen et al. (2000) presented a method that allowed the calculation of the lifetimes of tryptophan residues on the basis of spectral and structural data. In their article the authors determined an exponential relation between the nonradiative rate constant k_{nr} and the distance between the indole Cε3 atom and the carbonyl carbon of the peptide bond. This suggests a mechanism of electron transfer as the main determinant for the value of the nonradiative rate constant. This relation was based on the equation derived for electron transfer by Marcus and Sutin (1985). The authors used a molecular dynamics simulation map to identify the different rotamers of tryptophan. Further exploration of this method has to be done.

Here we report a new method to identify the different microconformations of tryptophan together with a method to link the rotamers with their respective lifetime on the basis of the correlation between the values of the rate constants for quenching with an external quencher (k_q) and the rotamer surface exposed to the solvent. In this study we use the dead-end elimination (DEE) method to determine the possible rotamers of tryptophan. This method is able to find the global optimal arrangement of a collection of side chains attached to a fixed main-chain structure (De Maeyer et al., 2000). The

---

Submitted November 17, 2002, and accepted for publication May 30, 2003.

Address reprint requests to Dr. Yves Engelborghs, Katholieke Universiteit Leuven, Laboratory of Biomolecular Dynamics, Celestijnenlaan 200D, 3001 Heverlee, Belgium. Tel.: 321-632-7160; Fax: 321-632-7974; E-mail: yves.engelborghs@fys.kuleuven.ac.be; or Dr. Marc De Maeyer, Katholieke Universiteit Leuven, Laboratory of Biomolecular Modelling, Celestijnenlaan 200D, 3001 Heverlee, Belgium. Tel.: 321-632-7521; Fax: 321-632-7974; E-mail: Marc.DeMaeyer@fys.kuleuven.ac.be.

0006-3495/03/09/1894/09 $2.00

DEE method detects and eliminates iteratively those rotamers that cannot be members of the Global Minimum Energy Conformation (GMEC; Desmet et al., 1992). The rotamer elimination occurs on the basis of energy criteria balancing rotamers against each other by comparing their main-chain interaction energy and a lower or higher limit for their interactions with the other side chains of the protein (De Maeyer et al., 2000). In this study the DEE method is applied on eight different proteins, whose single tryptophan mutants are available. The fact that the tryptophans of the eight proteins are buried inside the molecule strengthens the use of the DEE method to determine the possible rotamers of the Trp-residue. Indeed, it has been proven that the DEE method is quite accurate for buried residues (De Maeyer et al., 1997). The time-resolved fluorescence properties of the single tryptophan mutants of seven of these proteins have already been extensively investigated. These proteins, their tryptophan residues and the reference that describes them are listed in Table 1.

The eighth protein we use is trichosanthin (TCS). Trichosanthin from *Trichosanthes kirilowii*, a type I ribosome-inactivating protein is a monomeric 247-residue, 27,128 Da globular protein (Collins et al., 1990; Xiong et al., 1994). It contains a single tryptophan residue at position 192 that is buried inside the molecule (Zhang et al., 1993). The steady-state fluorescence properties of the Trp^{192} have been reported previously (Hao et al., 1995). Here we report the time-resolved fluorescence properties of TCS and a detailed quenching study with acrylamide to investigate the validity, in this case, of the proposed Hudson model. The values of k_q, which also reflect the accessible surface area (ASA) of tryptophan, provided us with a procedure to link the different rotamer clusters with their respective lifetime.

MATERIALS AND METHODS

Materials

Root tuber of *Trichosanthes kirilowii* (*TianHuaFen*) were obtained from a local drug store in China. All the chromatography materials were purchased from Pharmacia LKB. Acrylamide and *n*-acetyltryptophanamide (NATA) were purchased from Sigma Chemical (St Louis, MO). All other chemicals were of analytical grade. Distilled and deionized water was used throughout the experiments.

Protein purification

Trichosanthin was essentially purified as described previously (Zhang et al., 1993). The purity of the protein was examined by SDS-PAGE. The activity of the protein was determined by the method of Endo et al. (1987) by running the targeted RNA on a 1,2% agarose gel.

Multifrequency phase fluorometry

Fluorescence lifetimes were measured using automatic multifrequency phase fluorometry between 1.6 MHz and 1 GHz as described previously (Sillen et al., 2000). NATA in ddH$_2$O with a fluorescence lifetime of 3.059 ns (at 22°C) was used as reference. Data analysis was performed using a nonlinear least-squares algorithm (Bevington, 1969). Measurements performed at different emission wavelengths (320–380 nm) were analyzed simultaneously with global analysis to improve the recovery of lifetimes and amplitude fractions (Beechem et al., 1983). The data were fitted using the modified Levenberg-Marquardt algorithm (More and Sorensen, 1983) assuming that the fluorescence lifetimes are independent of the wavelength. This procedure allows the recovery of the fractional intensities with good accuracy.

Fluorescence quenching

The quenching of trichosanthin with increasing amounts of quencher was performed by adding aliquots of a freshly prepared 1-M acrylamide stock solution to the cuvette after which the changes in the fluorescence lifetimes and corresponding amplitude fractions were monitored. Fluorescence

TABLE 1 The used proteins, together with the position of the tryptophan residues, the PDB:IDs of the starting structures and mutations that have been made in the starting structures

Protein (PDB:ID)	Trp	Mutations	Reference(s)
Colicin A (1COL)	86	W130F/W140L/K113F	Vos et al. (1995)
	130	W86F/W140L/K113F	
	140	W86F/W130F	
DsbA (1FVK)	76	W126F	Hennecke et al. (1997)
	126	W76F	Sillen et al. (1999)
NSCP (2SCP)	4	W57F/W170F	Sillen et al. (2000)
	57	W4F/W170F	
	170	W4F/W57F	
Barnase (1A2P)	35	W71Y/W94F	Willaert et al. (1992)
	71	W35F/W94F	De Beuckeleer et al. (1999)
	94	W35F/W71Y	
PAI-I*	175	W86F/W139F/W262F	Verheyden et al. (2002)
	262	W86F/W139F/W175F	
Trichosanthin (1MRJ)	192	None	This article
Nuclease (1SNC)	140	None	Chen et al. (1987); Ababou and Bombarda (2001)
Ribonuclease T1 (9RNT)	59	None	Ababou and Bombarda (2001)

*A modeled structure is used.

lifetime as function of quencher concentration $[Q]$ was fitted by the classical Stern-Volmer equation,

$$1/\tau = 1/\tau_0 + (k_q \times [Q]), \tag{1}$$

where τ_0 (τ) is the lifetime in absence (presence) of quencher.

Starting structures

For each protein a full hydrogen model and energy minimized x-ray structure was used as the starting structure. For each structure only the monomer is taken into account. Some residues like Cys, HisH^+, Tyr, and Cystine are able to strongly quench fluorescence (Vos and Engelborghs, 1994; Chen and Barkley, 1998). Fluorescence data are available for single Trp-mutants of the eight proteins in which the neighboring quenching residues are mutated in nonquenching residues. Because we only take electron transfer to the peptide carbonyl into account, it is necessary to mutate in silico these neighboring quenching residues in the starting structures, so that it is possible to link the modeled structures with the experimental data. Table 1 shows the PDB:IDs of the starting structures and the mutations that have been made.

Dead-end elimination (DEE) method

To determine the possible conformations of tryptophan we used the dead-end elimination method. This method allows the determination of the GMEC of a side-chain collection in a fixed backbone configuration, using a side-chain rotamer library (Desmet et al., 1992). Tryptophan was placed in 1296 different starting values (for each χ-angle every 10°). Throughout this article, χ_1 is defined by the internal rotation around bond C_α-C_β and χ_2 by the bond C_β-C_γ. Within a shell of 8 Å around the fixed tryptophan, all side-chain residues were allowed to evolve. For each of the starting structures the GMEC was calculated with DEE. The backbone is kept fixed during the calculation. The rotamer library we used was an enhanced version of the libraries of De Maeyer et al. (1997). The energy parameters are based on the CHARMM force field (Brooks et al., 1983) but with reduced Van der Waals radii to account for small backbone movement (Gordon et al., 1999). For each GMEC, the nonbonded energy of tryptophan (E_{Trpnb}) in relation to the remaining structure of the protein and the total nonbonded energy (E_{totnb}) of the whole modeled protein was computed. The distance between the indole Cε3 atom and the carbonyl carbon of the peptide bond is also determined. The DEE algorithm has been implemented in the Brugel package (Delhaise et al., 1984). All calculations were performed on a single processor of a 4-processor Silicon Graphics Origin 2100 (R10000, 250 MHz).

Solvent-accessible area calculation

The solvent-accessible surfaces were calculated with the Survol option in the Brugel software package (Delhaise et al., 1984), using a probe sphere with a standard radius of 1.4 Å (Alard et and Wodak, 1991).

Determination of the radiative rate constant

Quantum yields were determined relative to tryptophan in water according to the method of Parker and Rees (1960):

$$Q_{\mathrm{Prot}} = \left[\left(\left(\int I_{\mathrm{Prot}} \times A_{\mathrm{Trp}}\right)/(I_{\mathrm{Trp}} \times A_{\mathrm{Prot}})\right] \times Q_{\mathrm{Trp}}, \tag{2}$$

where $\int I$ is the integrated intensity over the wavelength region 300–450 nm. A is the absorbance at 295 nm, and the quantum yield Q_{Trp} for tryptophan in water is taken as 0.14 (Kirby and Steiner, 1970).

The average radiative rate constant is calculated by dividing the quantum yield by a wavelength-independent amplitude average lifetime (Sillen and Engelborghs, 1998),

$$\langle k_r \rangle = Q/\sum \tau_i \alpha_i, \tag{3}$$

with $\sum \tau_i \alpha_i$ the average lifetime, α_i is a wavelength-independent amplitude fraction and is defined as (Sillen and Engelborghs, 1998),

$$\alpha_i = \left(\int I_{0i}(\lambda) d\lambda\right) / \left(\int I_0(\lambda) d\lambda\right). \tag{4}$$

The fluorescence intensity at time zero I_0 (λ) of each lifetime is integrated over the wavelength region 300–450 nm and then normalized.

Calculation of the nonradiative rate constant

The nonradiative rate constant (k_{nr}) is calculated as

$$k_{\mathrm{nr}} = (1/\tau) - k_r, \tag{5}$$

where k_r is the radiative rate constant, which is calculated as shown before, and τ is the fluorescence lifetime.

RESULTS

Identification of the tryptophan rotamers

The total nonbonded energies of the 1296 structures, as determined earlier, are sorted and only those with a negative E_{totnb} value are kept. This removes from the list of candidates all those with bad contacts. For the remaining structures a rough sorting is performed allowing only internal clashes below 36 kcal/mol. These structures might contain small, short contacts due to the discretization of the rotamer library. To alleviate these repulsions, the structures are further subjected to 100 steps of steepest descent energy minimization with fixed backbone. Because we are only interested in energetically low tryptophan rotamers, the remaining structures are sorted on basis of their E_{Trpnb} value as shown in Fig. 1 for the case of Trp^{130} of Colicin A. In agreement with Street and Mayo, (1999) we eliminate those structures where the Van der Waals energy of any atom pair exceeds a threshold of 3 kcal/mol, this is around the 125th structure.

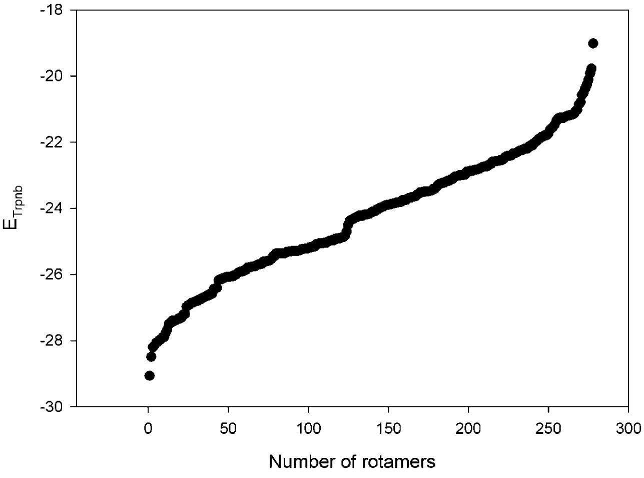

FIGURE 1 E_{Trpnb} profile of Trp^{130} of Colicin A.

The remaining structures represent approximately the best 25% of the energetically possible structures and provide us with clusters of Trp rotamer positions (see further). This procedure is repeated for each Trp of the eight modeled proteins.

Dead-end elimination

The rotamer clusters found for Trp^{130} of Colicin A are shown in Fig. 2. For each of the three observed clusters the mean distance between the indole Cε3 atom and the C atom of the peptide carbonyl is calculated. Table 2 shows the number and range of the rotamer clusters found for each modeled structure together with their mean distance between the indole Cε3 atom and the carbonyl carbon of the peptide bond. In most cases we find for tryptophan an equal number of rotamer clusters and fluorescence lifetimes.

Fluorescence lifetimes

The fluorescence decay of Trp^{192} in native TCS was measured at emission wavelengths ranging from 320 nm to 380 nm in 10-nm intervals. The decay curves were analyzed by single-curve analysis of the data at each wavelength and global analysis of data for seven emission wavelengths. The sum of two exponential terms was adequate to fit the data and yielded lifetime components of 1755 ns and a longer one of 4016 ns. Table 3 shows the results of the global fit for TCS.

Fluorescence quenching of TCS with acrylamide

The time-resolved fluorescence quenching by acrylamide was monitored to investigate the nature of the quenching mechanism. The effect of addition of acrylamide was not the same on the different lifetime components. Table 3 shows the results of quenching TCS with acrylamide. The two lifetimes show a linear dependence for the acrylamide concentration. Stern-Volmer plots for acrylamide quenching of the TCS lifetime components are shown in Fig. 3. The values for the bimolecular quenching constant k_q are 1.3 $\mathrm{M}^{-1} \pm 0.1$ M^{-1} ns^{-1} and 0.137 ± 0.06 M^{-1} ns^{-1} for τ_1 and τ_2, respectively. The value of k_q for the short lifetime component is 10-fold larger than that of the longer one, indicating that the short lifetime component is more solvent-accessible. For a fully exposed tryptophan residue (e.g., free Trp in water), k_q can be as high as 6.4 M^{-1} ns^{-1} (Vos et al., 1995). The ratio between α_1 and α_2 is shown in Table 4 and remains practically constant during the quenching experiment.

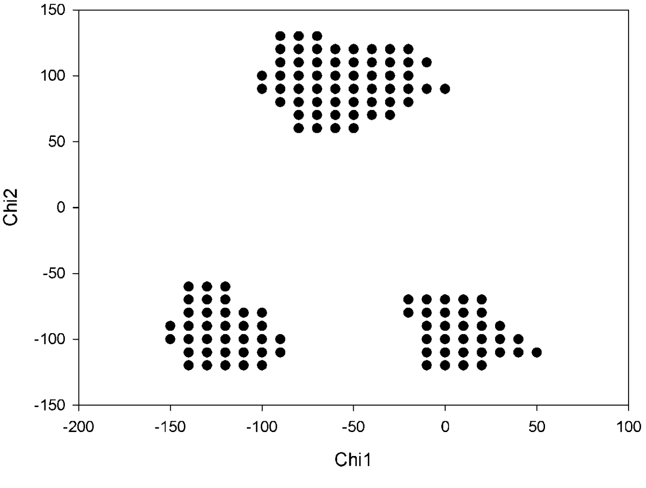

FIGURE 2 Rotamer clusters found for Trp^{130} of Colicin A, using the Van der Waals cutoff value of 3 kcal/mol.

Accessible surface area

The ASA for a fully exposed Trp is 264 Å. Table 5 shows the surface-accessible areas for every Trp in the x-ray structure. The ASA for every rotamer cluster of Trp^{192} of TCS and the three tryptophans of colicin A are shown in Table 6.

DISCUSSION

The fluorescence decay of the single tryptophan residue in trichosanthin is double-exponential. For T4-lysozyme, a single Trp protein which also shows a double-exponential decay, Hudson (1999) proposed a new model. In this model it is assumed that reversible electron transfer can occur between tryptophan and a neighboring amino acid side chain. This mechanism gives rise to two exponentials: Eq. 6, where the amplitudes are determined in a complex way by the different rate constants involved; and Eq. 7.

$$\begin{array}{ccc} W^* + Q & \underset{k_{\mathrm{AB}}}{\overset{k_{\mathrm{BA}}}{\rightleftarrows}} & (W^{*+})(Q^{*-}) \\ k_{\mathrm{A0}}\downarrow & & \downarrow k_{\mathrm{B}} \\ W & \rightleftarrows & H \end{array} \tag{6}$$

$$W^*(t) = \alpha \exp(-k_1 t) + (1-\alpha)\exp(-k_2 t),$$

with

$$\begin{aligned} k_{1,2} = {} & [(k_{\mathrm{A0}} + k_{\mathrm{AB}} + k_{\mathrm{B}} + k_{\mathrm{BA}}) \\ & \pm [(k_{\mathrm{A0}} + k_{\mathrm{AB}} - k_{\mathrm{B}} - k_{\mathrm{AB}})^2]^{1/2}]/2. \end{aligned}$$

W* is the excited tryptophan residue which decays to the ground state W by both radiative and nonradiative processes ($k_{\mathrm{A0}} = k_{\mathrm{r}} + k_{\mathrm{nr}}$). k_{AB} and k_{BA} are respectively the rate constants of the forward and reverse electron transfer reaction. Q is a collisional electron acceptor and H is either the ground state of tryptophan or another low-energy species (e.g., the triplet state; Hudson, 1999):

$$\alpha/(1-\alpha) = (k_{\mathrm{A0}} + k_{\mathrm{AB}} - k_2)/(k_1 - (k_{\mathrm{A0}} + k_{\mathrm{AB}})). \tag{7}$$

When we fill in the results of the fluorescence lifetime measurements of trichosanthin with no acrylamide present, we find a value of 0.2926 for ($k_{\mathrm{A0}} + k_{\mathrm{AB}}$). If Hudson's model

TABLE 2 Rotamer clusters for the tryptophans of the eight used proteins

Trp (protein)	Rotamer cluster	χ_1	χ_2	Mean distance (Å)
W86 (Colicin A)	1	−60; −30	130; 170	4.09
	2	−40; −110	80; 150	4.72
	3	−90; −110	−60; −120	5.38
W130 (Colicin A)	1	−100; 0	60; 130	4.10
	2	−150; −90	−60; −120	5.00
	3	−20; 50	−70; −120	4.88
W140 (Colicin A)	1	−80; −40	10; −60	5.51
	2	−80; −40	120; 180	4.59
W35 (Barnase)	1	150; 170; −180; −160	30; 110	4.19
	2	120; 150	−60; −90	4.94
W71 (Barnase)	1	−60; 0	−70; −120	4.61
	2	−30; −10	100; 130	5.08
	3	−80; −60	70; 120	4.75
W94 (Barnase)	1	−60; 0	90; 120	4.80
	2	−70; 20	−10; −100	5.39
	3	50; 60	−90; −110	4.46
	4	50; 100	40; 90	5.29
W76 (DsbA)	1	−130; −90	30; 60	5.11
	2	−170; −100	100; 150	4.41
	3	150; 170; −180; −140	−40; −160	3.67
W126 (DsbA)	1	−170; −120	50; 110	4.53
	2	−160; −120	20; −10	5.00
	3	150; 170; −180; −160	−60; −120	3.80
W192 (Trichosanthin)	1	−150; −180; 170; 140	10; 80	4.80
	2	80; 150	−80; −50	4.36
W57 (NSCP)	1	−180; −120; 80; 170	−50; −140	4.44
	2	−180; −120; 80; 170	40; 160	3.72
W4 (NSCP)	1	−140; −180; 170; 160	0; 110	3.37
	2	120; 170	−40; −150	4.44
W170 (NSCP)	1	−100; −30	50; 170	4.80
	2	−140; −70	−50; −150	5.15
W262 (PAI-I)	1	−80; −40	150; 170; −140; −180	4.61
	2	−110; −40	20; −90	5.61
W175 (PAI-I)	1	−90; −30	110; 180	4.66
	2	−50; −130	0; 120	5.15
W59 (RNT1)	1	−160; −140	60; 110	3.80
	2	−170; −180; 170; 130	−140; −60	4.57
W140 (Nuclease)	1	−110; −10	70; 160	4.60
	2	−160; −120	−90; −130	4.92
	3	−70; −110	−50; −110	5.42

would be applicable on TCS, then adding an external quencher Q_{ext}, e.g., acrylamide would change the ratio of the amplitudes, as in

$$\alpha/(1-\alpha) = (k_{A0} + k_{qA}[Q_{ext}] + k_{AB} - k_2)/(k_1 - (k_{A0} + k_{qA}[Q_{ext}] + k_{AB})), \tag{8}$$

with k_{qA} the bimolecular quenching constant of acrylamide on the excited state of tryptophan.

The quenching experiments we performed provide us with values for k_1, k_2, and k_{qA}. Together with the value of 0.2926 for ($k_{A0} + k_{AB}$), we can calculate the ratio of the amplitudes for each concentration of acrylamide, in which case Hudson's model would be valid for TCS. These values are shown

TABLE 3 Fluorescence lifetimes and amplitude fractions of the Trp^{192} in trichosanthin; the measurements were performed at 20°C

α_1	τ_1 (ns)	α_2	τ_2 (ns)	χ^2	Acrylamide (M)
0.136 ± 0.018	1.755 ± 0.175	0.864 ± 0.105	4.016 ± 0.042	1.402	0.000
0.108 ± 0.009	1.325 ± 0.150	0.892 ± 0.074	3.842 ± 0.031	1.808	0.050
0.125 ± 0.01	1.443 ± 0.123	0.875 ± 0.070	3.757 ± 0.035	1.578	0.100
0.124 ± 0.008	1.150 ± 0.105	0.876 ± 0.057	3.543 ± 0.023	1.421	0.200
0.128 ± 0.006	0.988 ± 0.092	0.872 ± 0.041	3.371 ± 0.028	1.859	0.300
0.141 ± 0.007	0.950 ± 0.085	0.859 ± 0.043	3.241 ± 0.025	1.680	0.400
0.161 ± 0.009	1.003 ± 0.092	0.839 ± 0.047	3.150 ± 0.036	1.789	0.500

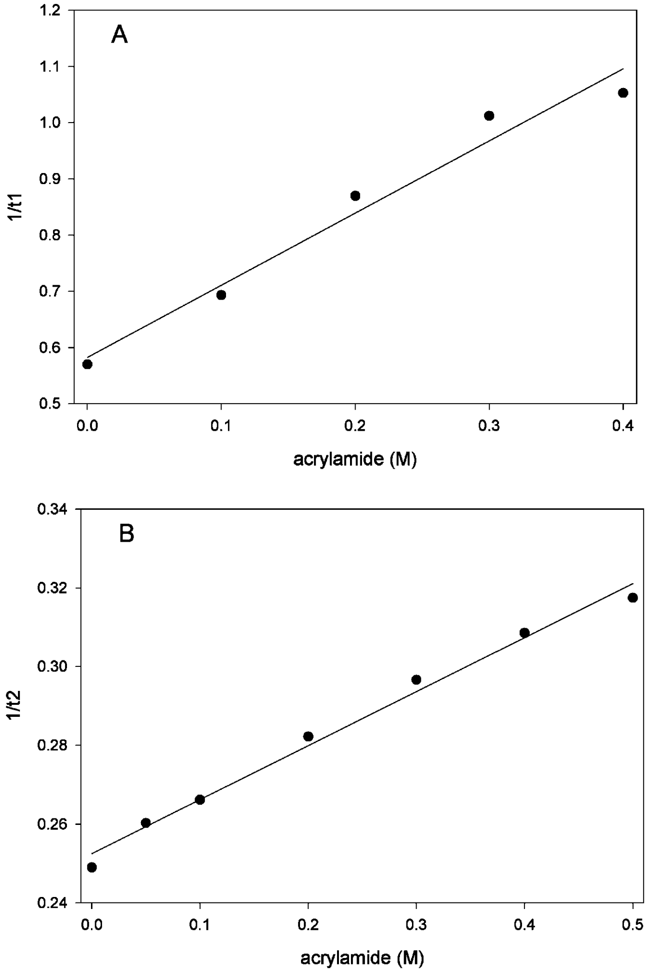

FIGURE 3 Acrylamide quenching of tryptophan fluorescence of TCS. (*A*) Stern-Volmer plot for the shortest lifetime component. (*B*) Stern-Volmer plot for the longest lifetime component.

in Table 4. We clearly see that the ratio of the amplitudes should raise upon addition of acrylamide. However, in our experiments the ratio of the amplitudes remains practically constant (see Table 4). We therefore can exclude reversible electron transfer in this case. We can explain the results by the existence of different rotamers of Trp, where the amplitudes reflect populations of different rotamers. These ground-state rotamers are the result from rotations about the C_α-C_β and C_β-C_γ bonds. Each rotamer has a specific local environment with different distances and/or orientations to quencher groups, yielding distinct nonradiative decay rates. Since the Trp fluorescence is not damaged upon radiation, electron transfer has to be reversible. The fact that the Hudson model is not applicable for this protein indicates that the reverse reaction is much slower than the nanosecond timescale. Usually reverse electron transfer reactions are orders-of-magnitude smaller than forward reactions (Mataga et al., 1988a,b; Paddon-Row et al.,1988). For the other proteins we did not eliminate the possibility of fast reversible electron transfer, but on the basis of the reasoning above we think it is very unlikely.

TABLE 4 Ratio between the amplitude fractions

α_1/α_2	α_1/α_2 for Hudson's model
0.157 ± 0.028	0.157
0.121 ± 0.014	0.245
0.143 ± 0.016	0.579
0.142 ± 0.013	0.853
0.147 ± 0.010	1.171
0.164 ± 0.012	2.100
0.192 ± 0.015	11.490

TABLE 5 Accessible surface areas of each tryptophan residue in the PDB structure

Protein	Trp	Accessible surface area (Å^2)
Colicin A	86	1.0
	130	7.5
	140	9.9
DsbA	76	3.0
	126	47.2
NSCP	4	1.2
	57	6.5
	170	1.0
Barnase	35	11.8
	71	5.6
	94	70.5
Pai-I	175	2.8
	262	2.7
Trichosanthin	192	15.6
Ribonuclease T1	59	1.0
Nuclease	140	73.0

Except for the case of the two tryptophans in NSCP, the number of rotamer clusters found for a tryptophan residue is equal to the number of Trp fluorescence lifetimes. The challenge is to find a procedure to link the rotamer clusters with their respective lifetimes. In this case we are able to link 10 lifetimes with 10 rotamers. To link to the rotamer clusters with their fluorescence lifetimes, we calculated the accessible surface area of the clusters and compared them with the values of the bimolecular quenching constants. In the case of trichosanthin, we find two rotamer clusters, one with an ASA

TABLE 6 ASA for W192 of TCS, W86, W130, and W140 of Colicin A

Trp (protein)	Rotamer cluster	ASA (Å^2)
W86 (Colicin A)	1	0.55
	2	0.27
	3	0.34
W130 (Colicin A)	1	13.89
	2	7.1
	3	59.67
W140 (Colicin A)	1	15.93
	2	55.89
W192 (TCS)	1	3.046
	2	13.481

of 13.5 Å^2 and another with an ASA of 3.0 Å^2, as shown in Table 6. The quenching experiments with acrylamide yield two bimolecular quenching constants and indicate that the short lifetime is more solvent-accessible. According to these results the cluster with the highest ASA should be linked with the short fluorescence lifetime of tryptophan. If we compare the accessible areas of the tryptophans of Colicin A (Table 6) with the bimolecular quenching constants found in quenching experiments with acrylamide of these tryptophans (Table 3, Vos et al., 1995) we see the same similarity as in the case of trichosanthin. In this set of 10 rotamers we also observed that the short lifetimes correlate with a short distance between Cε3 and the peptide carbonyl C atom, in agreement with the mechanism of electron transfer proposed by Marcus and Sutin. Because of this observed relation, we linked the 40 found rotamer clusters for Trp of the eight proteins with their respectable lifetimes in the same way. In the future, additional quenching experiments of those proteins where up to now no acrylamide quenching has been performed, can further confirm the match between both methods.

Recently, the quantum yield was correlated to the environment of the tryptophan in the protein, i.e., the electric field, by using quantum mechanical calculations (Callis and Vivian, 2003). Although these calculations provide the most general answer, we try here to find out if the exponential relation for electron transfer, as proposed by Marcus and Sutin (1985), and as attempted before (Sillen et al., 2000), can be applied. It should be noted that the tryptophan residues we study in this sample are selected for the absence of special features like quenching groups, charge, stacked, or perpendicular aromatic groups.

The radiative rate constant is experimentally determined for all the proteins from the quantum yield and the average fluorescence lifetime. The knowledge of both the fluorescence lifetime and radiative rate constant for each rotamer cluster makes it possible to calculate the nonradiative rate constant for each rotamer cluster with Eq. 5.

These nonradiative rate constants are fitted to their respective distance between Cε3 of Trp and the carbonyl carbon of the peptide bond by the following equation, derived for electron transfer by Marcus and Sutin:

$$k_{\mathrm{et}}(R) = k_0 \exp(-\beta(R - R_0), \tag{9}$$

where k_{et} (R) is the rate for electron transfer, k_0 is the rate of electron transfer at the Van der Waals contact distance ($R_0 =$ 3 Å), β is the range parameter that is depended on the medium. Fluorescence lifetime measurements show an experimental error, and because k_{nr} is calculated on the basis of these lifetime measurements, this error will stay. Therefore, we use a weighted-fit with weight factors given as follows:

$$\text{Weight factor} = k_{\mathrm{nr}}/S_{\mathrm{knr}}, \tag{10}$$

with S_{knr} the standard deviation of k_{nr}, as shown in Eq. 10,

$$S_{\mathrm{knr}} = [(S_\tau/\tau^2)^2 + (S_{\mathrm{kr}})^2]^{1/2}, \tag{11}$$

And with S_τ the standard deviation of the fluorescence lifetime τ and S_{kr} the standard deviation of the radiative rate constant k_{r}. This fit yields a value of 5.046 ± 0.335 ns^{-1} for k_0 and a value of 1.497 ± 0.074 Å^{-1} for β and is shown in Fig. 4.

If we compare these values with the value of 25 ± 3 ns^{-1} for k_0 and 1.9 ± 0.1 Å^{-1}, determined by Sillen et al. (2000) (with only four data points), we see that both parameters are smaller. Recently Laboulais et al. (2001) simulated the fluorescence decay of the tryptophans in the HIV-1 integrase catalytic core. Among the many possible quenching processes, they only took the quenching by the peptide bond into account using the formula of Sillen et al. (2000). In their work, the best fits were obtained with a value for $\beta \sim 1.9$ Å^{-1} in agreement with Sillen et al. (2000). In contrast the electron transfer rate constant k_0 had to be lowered from 25 ns^{-1} (Sillen et al., 2000) to a value ~3.7 ns^{-1}. Adams et al. (2002) recently published a value of 330 ns^{-1} for the pre-exponential factor, B of NATA, using a β-value of 1.7 Å^{-1} (Beratan et al., 1991), and assuming that there is no orientation dependency. If they take the orientation dependence into account, this value raises to 1100 ns^{-1}. Translation of this pre-exponential factor B (with $R_0 = 0$ Å) to a k_0 (with $R_0 = 3$ Å) value is what we use in formula 4, which gives a value of 2.03 ns^{-1} for k_0 with no orientation dependency and a value of 6.1 ns^{-1} for k_0 with orientation dependency. The k_0 value of 5 ns^{-1} that we determined approximates the k_0 values determined by Laboulais et al. (2001) and Adams et al. (2002). The experimental correlation that we observe in this way, linking the nonradiative rate constant and the rotamer conformation, can be used to predict the lifetime in the absence of any special

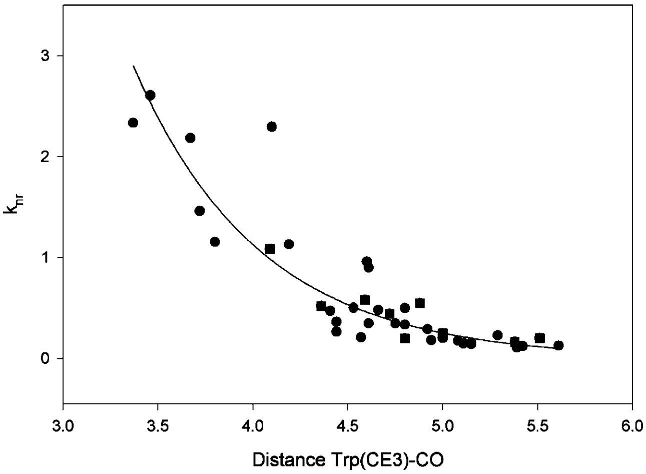

FIGURE 4 The nonradiative rate constant as function of the distance between the Cε3 atom of Trp and the C atom of the peptide carbonyl. ■, 10 datapoints for which the relation between k_{q} and ASA could be determined. ●, 30 datapoints assigned on the basis of the relation of short-lifetime, short Cε3-C=O distance.

feature. It is clear that only a quantum mechanical calculation can give a more general answer.

For Ribonuclease T1, using molecular mechanics (Ababou and Bombarda, 2001) only identified one tryptophan rotamer and therefore these authors rejected the rotamer model. This in contrast with the two rotamers revealed here by the DEE method. Contrary to other methods like energy minimization, molecular mechanics, or molecular dynamics, the DEE method explores the complete conformational space and detects the GMEC. The classic method of an energy map cannot explore all possible rotamer combinations by brute force. As an example, a Trp in contact with six other residues (having only two rotatable χ-angles) and allowing χ-angle deviations in steps of 10° explodes into 6.10^{21} possible conformations. If one rotamer calculation takes 1 ms, the total exploration of the conformational space would require 2.10^{11} years. In addition, molecular dynamics runs are in general too short to be sure that all possible energy minima are visited. If we compare the energy minima we find with DEE for Trp^{57} in NSCP with those determined by a molecular dynamics simulation performed by Sillen et al. (2000), we can see that the two most populated conformations are found with both techniques.

CONCLUSION

In conclusion it can be stated that for 10 lifetimes we were able to obtain a fully objective identification of the corresponding rotamer, on the basis of the correlation between the quenching constant (k_q) and the accessible surface. For these points of data the relation holds that a short lifetime corresponds to short Cε3-C=O distance, suggesting the electron transfer mechanism. Therefore the same correlation was used to identify the rotamers of 30 additional lifetimes. The whole set of 40 datapoints allows us to determine a good average of k_0 and β. Only for the tryptophans of NSCP is an additional lifetime found, which might be an indication for additional sources of heterogeneity.

This research is supported by the National Fund for Scientific Research of the Flanders (project G-0092-01).

REFERENCES

Ababou, A., and E. Bombarda. 2001. On the involvement of electron transfer reactions in the fluorescence decay kinetics heterogeneity of proteins. *Protein Sci.* 10:2102–2113.

Adams, P. D., Y. Chen, K. Ma, M. G. Zagorski, F. D. Sönnichsen, M. L. McLaughin, and M. D. Barkley. 2002. Intramolecular quenching of tryptophan fluorescence by the peptide bond in cyclic hexapeptides. *J. Am. Chem. Soc.* 124:9278–9286.

Alard, P., and S. J. Wodak. 1991. Detection of cavities in a set of interpenetrating spheres. *J. Comput. Chem.* 12:918–922.

Antonini, P. S., W. Hillen, N. Ettner, W. Hinrichs, P. Fantucci, S. M. Doglia, J.-A. Bousquet, and M. Chabbert. 1997. Molecular mechanics analysis of Tet repressor Trp43 fluorescence. *Biophys. J.* 72:1800–1811.

Bajzer, Z., and F. G. Prendergast. 1993. A model for multi-exponential tryptophan fluorescence intensity decay in proteins. *Biophys. J.* 65:2313–2323.

Beechem, J. M., J. R. Knutson, J. B. A. Ross, B. W. Turner, and L. Brand. 1983. Global resolution of heterogeneous decay by phase modulation fluorometry: mixtures and proteins. *Biochemistry.* 22:6054–6058.

Beratan, D. N., J. N. Betts, and J. N. Onuchic. 1991. Protein electron transfer rates set by the bridging secondary and tertiary structure. *Science.* 252:1285–1288.

Bevington, P. R. 1969. Gradient-expansion algorithm. *In* Data Reduction and Error Analyses for the Physical Sciences. McGraw-Hill, New York. pp.235–240.

Brooks, B. R., R. E. Bruccoleri, B. D. Olafson, D. J. States, S. Swaminathan, and M. Karplus. 1983. CHARMM: a program for molecular energy, minimization, and dynamics calculations. *J. Comput. Chem.* 4:187–217.

Brown, M. P., and C. Royer. 1997. Fluorescence spectroscopy as a tool to investigate protein interactions. *Curr. Opin. Biotechnol.* 8:45–49.

Callis, P. R., and J. T. Vivian. 2003. Understanding the variable fluorescence quantum yield of tryptophan in proteins using QM-MM simulations. Quenching by charge transfer to the peptide backbone. *Chem. Phys. Lett.* 369:409–414.

Chang, M. W., J. W. Petrich, D. B. McDonald, and G. R. Fleming. 1983. Nonexponential fluorescence decay of tryptophan and N-terminal tryptophyl peptides. *J. Am. Chem. Soc.* 105:3819–3824.

Chen, Y., H. T. Yu, and M. D. Barkley. 1996. The peptide bond quenches indole fluorescence. *J. Am. Chem. Soc.* 118:9271–9278.

Chen, Y., and M. D. Barkley. 1998. Toward understanding tryptophan fluorescence in proteins. *Biochemistry.* 37:9976–9982.

Collins, E. J., J. D. Robertus, M. LoPresti, K. L. Stone, K. R. Williams, P. Wu, K. Hwang, and M. Piatak. 1990. Primary amino acid sequence of alpha-trichosanthin and molecular models for abrin A-chain and alpha-trichosanthin. *J. Biol. Chem.* 265:8665–8669.

Dahms, T. E. S., K. J. Willis, and A. G. Szabo. 1995. Conformational heterogeneity of tryptophan in a protein crystal. *J. Am. Chem. Soc.* 117:2321–2326.

De Beuckeleer, K., G. Volckaert, and Y. Engelborghs. 1999. Time-resolved fluorescence and phosphorescence properties of the individual tryptophan residues of barnase: evidence for protein-protein interactions. *Protein Struct. Funct. Gen.* 36:42–53.

Delhaise, P., M. Bardiaux, and S. Wodak. 1984. Interactive computer animation of macromolecules. *J. Mol. Graph.* 2:103–106.

Desmet, J., M. De Maeyer, B. Hazes, and I. Lasters. 1992. The dead-end elimination theorem and its use in protein side-chain positioning. *Nature.* 356:539–542.

De Maeyer, M., J. Desmet, and I. Lasters. 1997. All in one: a highly detailed rotamer library improves both the accuracy and speed in the modelling of sidechains by dead-end elimination. *Fold. Des.* 2:53–66.

De Maeyer, M., J. Desmet, and I. Lasters. 2000. The dead-end elimination theorem: mathematical aspects, implementation, optimizations, evaluation, and performance. *Methods Mol. Biol.* 143:265–304.

Endo, Y., K. Mitsui, M. Motizuki, and K. Tsurugi. 1987. The mechanism of action of ricin and related toxic lectins on eukaryotic ribosomes. The site and the characteristics of modification in 28 S ribosomal RNA caused by the toxins. *J. Biol. Chem.* 262:5908–5912.

Goldman, C., P. G. Pascutti, P. Piquini, and A. S. Ito. 1995. On the contribution of electron transfer reactions to quenching of tryptophan fluorescence. *J. Chem. Phys.* 103:10614–10620.

Gordon, D. B., S. A. Marshall, and S. L. Mayo. 1999. Energy functions for protein design. *Curr. Opin. Struct. Biol.* 9:509–513.

Hao, Q., Y. Zhang, H. Yang, G. Liu, Z. Huang, B. Liu, Q. Yao, and Q. Li. 1995. Fluorescence spectroscopic study of the interaction of adenine and nucleotide with trichosanthin. *Biochem. Mol. Biol. Int.* 36:889–895.

Hennecke, J., A. Sillen, M. Huber-Wunderlich, Y. Engelborghs, and R. Glockshuber. 1997. Quenching of tryptophan fluorescence by the active-site disulfide bridge in the DsbA protein from *Escherichia coli*. *Biochemistry*. 36:6391–6400.

Hudson, B. S. 1999. An ionization/recombination mechanism for complexity of the fluorescence of tryptophan in proteins. *Acc. Chem. Res.* 32:297–300.

Kirby, E. P., and R. F. S. Steiner. 1970. The influence of solvent and temperature upon the fluorescence of indole derivatives. *J. Phys. Chem.* 74:4480–4490.

Laboulais, C., E. Deprez, H. Leh, J. F. Mouscadet, J. C. Brochon, and M. Le Bret. 2001. HIV-1 integrase catalytic core: molecular dynamics and simulated fluorescence decays. *Biophys. J.* 81:473–489.

Marcus, R. A., and N. Sutin. 1985. Electron transfer in chemistry and biology. *Biochim. Biophys. Acta.* 811:265–322.

Mataga, N., Y. Kanda, T. Asahi, H. Miyasaka, T. Okada, and T. Kakitani. 1988a. Mechanisms of the strongly exothermic charge separation reaction in the excited singlet-state-picosecond laser photolysis studies on aromatic hydrocarbon tetracyanoethylene and aromatic hydrocarbon pyromellitic dianhydride systems in polar solutions. *Chem. Phys.* 127:239–248.

Mataga, N., T. Asahi, Y. Kanda, T. Okada, and T. Kakitani. 1988b. The bell-shaped energy-gap dependence of the charge recombination reaction of geminate radical ion-pairs produced by fluorescence quenching reaction in acetonitrile solution. *J. Phys. Chem.* 88:5138–5145.

Milner-White, E. J. 1997. The partial charge of the nitrogen atom in peptide bonds. *Protein Sci.* 6:2477–2482.

More, J. J., and D. C. Sorensen. 1983. Computing a trust region step. *SIAM J. Sci. Stat. Comput.* 4:553–572.

Paddon-Row, M. N., A. M. Oliver, J. M. Warman, K. J. Smit, M. P. Dehaas, H. Oevering, and J. W. Verhoeven. 1988. Factors affecting charge separation and recombination in photoexcited rigid donor insulator acceptor compounds. *J. Phys. Chem.* 92:9658–9662.

Ricci, R. W., and J. M. Nesta. 1976. Inter- and intramolecular quenching of indole fluorescence by carbonyl compounds. *J. Phys. Chem.* 80:974–980.

Parker, C. A., and W. T. Rees. 1960. Corrections of fluorescence spectra and the measurement of fluorescence quantum efficiency. *Analyst.* 85:587–600.

Sillen, A., and Y. Engelborghs. 1998. The correct use of ''average'' fluorescence parameters. *Photochem. Photobiol.* 67:475–486.

Sillen, A., J. Hennecke, D. Roethlisberger, R. Glockshuber, and Y. Engelborghs. 1999. Fluorescence quenching in the DsbA protein from *Escherichia coli*: complete picture of the excited-state energy pathway and evidence for the reshuffling dynamics of the microstates of tryptophan. *Protein Struct. Funct. Gen.* 37:253–263.

Sillen, A., J. F. Díaz, and Y. Engelborghs. 2000. A step toward the prediction of the fluorescence lifetimes of tryptophan residues in proteins based on structural and spectral data. *Protein Sci.* 9:158–169.

Street, A. G., and S. L. Mayo. 1999. Intrinsic β-sheet propensities result from van der Waals interactions between side chains and the local backbone. *Proc. Natl. Acad. Sci. USA.* 96:9074–9076.

Szabo, A. G., and D. M. Rayner. 1980. Fluorescence decay of tryptophan conformers in aqueous solution. *J. Am. Chem. Soc.* 102:554–563.

Vos, R., and Y. Engelborghs. 1994. A fluorescence study of tryptophan-histidine interaction in the peptide anantin and in solution. *Photochem. Photobiol.* 60:24–32.

Vos, R., Y. Engelborghs, J. Izard, and D. Baty. 1995. Fluorescence study of the three tryptophan residues of the pore-forming domain of Colicin A using multifrequency phase fluorometry. *Biochemistry.* 35:1734–1743.

Willaert, K., R. Loewenthal, J. Sancho, M. Froeyen, A. R. Fersht, and Y. Engelborghs. 1992. Determination of the excited-state lifetimes of the tryptophan residues in barnase, via multifrequency phase fluorometry of tryptophan mutants. *Biochemistry.* 31:711–716.

Xiong, J. P., Z. X. Xia, and Y. Wang. 1994. Crystal structure of trichosanthin-NADPH complex at 1.7 Å resolution reveals active-site architecture. *Nat. Struct. Biol.* 1:695–700.

Zhang, Y., W. Li, Q. Hao, G. Yu, Q. Li, and Q. Yao. 1993. Tb(III) and Eu(III) as fluorescent probes to investigate the metal-binding sites of trichosanthin. *Biochem. Biophys. Res. Commun.* 197:407–414.